Original research   http://dx.doi.org/10.1016/j.apjtm.2017.05.012

Rosmarinic acid attenuates hepatic fibrogenesis via suppression of hepatic stellate cell activation/proliferation and induction of apoptosis

Naglaa M. El-Lakkany[1✉], Walaa H. El-Maadawy[1], Sayed H. Seif el-Din[1], Olfat A. Hammam[2], Salwa H. Mohamed[3], Shahira M. Ezzat[4], Marwa M. Safar[5], Samira Saleh[5]

[1]Department of Pharmacology, Theodor Bilharz Research Institute, Warak El-Hadar, Imbaba P.O. Box 30, Giza 12411, Egypt

[2]Department of Pathology, Theodor Bilharz Research Institute, Warak El-Hadar, Imbaba P.O. Box 30, Giza 12411, Egypt

[3]Department of Immunology, Theodor Bilharz Research Institute, Warak El-Hadar, Imbaba P.O. Box 30, Giza 12411, Egypt

[4]Department of Pharmacognosy, Faculty of Pharmacy, Cairo University, Cairo 11562, Egypt

[5]Department of Pharmacology and Toxicology, Faculty of Pharmacy, Cairo University, Cairo 11562, Egypt

ARTICLE INFO

ABSTRACT

Objective: To investigate the antifibrotic role of rosmarinic acid (RA), a natural polyphenolic compound, on HSCs activation/proliferation and apoptosis *in vitro* and *in vivo*.
Methods: The impact of RA on stellate cell line (HSC-T6) proliferation, activation and apoptosis was assessed along with its safety on primary hepatocytes. *In vivo*, rats were divided into: (i) normal; (ii) thioacetamide (TAA)-intoxicated rats for 12 weeks; (iii) TAA + silymarin or (iv) TAA + RA. At the end of experiment, liver functions, oxidative stress, inflammatory and profibrogenic markers, tissue inhibitor metalloproteinases type-1 (TIMP-1) and hydroxyproline (HP) levels were evaluated. Additionally, liver histopathology and immunohistochemical examinations of alpha-smooth muscle actin (α-SMA), caspase-3 and proliferation cellular nuclear antigen (PCNA) were determined.
Results: RA exhibited anti-proliferative effects on cultured HSCs in a time and concentration dependent manner showing an IC_{50} of 276 µg/mL and 171 µg/mL for 24 h and 48 h, respectively, with morphological reversion of activated stellate cell morphology to quiescent form. It significantly improved ALT, AST, oxidative stress markers and reduced TIMP-1, HP levels, inflammatory markers and fibrosis score (S1 *vs* S4). Furthermore, reduction in α-SMA plus elevation in caspase-3 expressions of HSCs *in vitro* and *in vivo* associated with an inhibition in proliferation of damaged hepatocytes were recorded.
Conclusions: RA impeded the progression of liver fibrosis through inhibition of HSCs activation/proliferation and induction of apoptosis with preservation of hepatic architecture.

1. Introduction

Liver fibrosis and its end-stage cirrhosis are major causes of morbidity and mortality worldwide. Liver fibrosis is not an independent disease but rather a sequel of chronic liver diseases including viral hepatitis, alcoholic or nonalcoholic fatty liver disease, autoimmune hepatitis and parasitic infection [1]. Preventing or inhibiting the progression of fibrosis may reduce the economic burden and, more importantly, the decline in health-related quality of life [2].

Hepatic stellate cells (HSCs) play a crucial role in the progression and resolution of hepatic fibrosis [3]. In normal liver, HSCs store retinoids and vitamin A [4], whereas upon injury they become activated and trans-differentiated into myofibroblast-like cells. Such trans-differentiation is provoked by cytokines release including transforming growth factor (TGF)-β1,

✉First and corresponding author: Naglaa M. El-Lakkany, Department of Pharmacology, Theodor Bilharz Research Institute, Warak El-Hadar, Imbaba P.O. Box 30, Giza 12411, Egypt.
    Tel: +20 1223329483
    Fax: +20 2 3540 8125
    E-mails: n.ellakkany@tbri.gov.eg, naglaaellakkany@gmail.com
    Peer review under responsibility of Hainan Medical University.

platelet derived growth factor (PDGF) and tumor necrosis factor-α (TNF-α) complemented with boosted proliferation and expression of α-smooth muscle actin (α-SMA), loss of vitamin A stores plus overproduction of extracellular matrix (ECM) [3] thereby accelerating the progression of liver fibrosis [5].

Despite the extensive knowledge of the mechanisms underlying hepatic fibrosis, so far the potent and effective anti-fibrotic drug remains indefinable [6]. Currently, developing drugs from natural products have driven worldwide attention [7] for being safe and cost-effective making them potential anti-fibrotic agents. However, for many natural products, the mechanism of action is still unknown thus impeding drug development [8].

Rosmarinic acid (a-O-caffeoyl-3,4-dihydroxyphenyllactic acid; RA), a naturally occurring hydroxylated compound, is commonly found in various plants from *Lamiaceae* family including *Rosmarinus officinalis* (*R. officinalis*) (rosemary) [9]. RA has a variety of salutary biological activities including anti-inflammatory [10], antioxidant [11], antiangiogenic [12] and anticancer [13] activities. Consequently, this study provides insights on the antifibrotic effects of RA through focusing mainly on HSCs both in *vitro* and in a rat model of thioacetamide (TAA)-induced fibrosis.

2. Materials and methods

2.1. Drug and reagents

Tissue inhibitor metalloproteinases, type 1 (TIMP-1), platelet derived growth factor-BB (PDGF-BB) and tumor growth factor-β1 (TGF-β1) ELISA kits were purchased from Quantikine R&D systems (Minneapolis, USA). Serum alanine and aspartate aminotransferases kits were purchased from Spectrum (Cairo, Egypt). Dimethyl sulphoxide (DMSO), collagenase Type IV, thiazolyl blue tetrazolium bromide (MTT), sulforhodamine base (SRB), thioacetamide, 5,5′-dithiobis-2-nitrobenzoic acid (Ellman's reagent), chloramine T, 4-dimethylaminobenzaldehyde (Ehrlich reagent), standard hydroxyproline (HP), standard reduced glutathione were purchased from Sigma–Aldrich Chemical Co. (MO, USA). Anti-Interleukin (IL)-6, anti-lymphocyte common antigen (CD45), anti-caspase-3, anti-alpha smooth muscle actin (α-SMA) and anti-proliferating cell nuclear antigen (PCNA) monoclonal antibodies, mouse and rabbit specific HRP/DAB detection IHC kits were purchased from Santa Cruz Biotechnology (CA, USA). Silymarin (Legalon®) was purchased from Chemical Industries Development, CID (Cairo, Egypt). All other chemicals and solvents were of the highest grade commercially available.

2.2. Plant materials

The aerial parts of *R. officinalis* L. were obtained from the experimental station of medicinal, aromatic and poisonous plants, Pharmacognosy Department, Faculty of Pharmacy, Cairo University, Cairo, Egypt in spring 2014 and was kindly authenticated by Prof. Dr. Wafaa Amer, Botany Department, Faculty of Science, Cairo University, Giza, Egypt. A voucher specimen (2014067) was kept in the herbarium of the Pharmacognosy Department, Faculty of Pharmacy, Cairo University.

2.3. Extraction and isolation of RA

One kilogram of the powdered air-dried aerial parts of *R. officinalis* was extracted with methanol in a soxhlet until exhaustion. The methanolic extract was concentrated under reduced pressure to yield 200 g of the dry residue, which was suspended in distilled water (700 mL) and defatted by partition with methylene chloride (3 × 500 mL). The mother liquor was then fractionated over Diaion HP-20 using water, 50% methanol in water and 100% methanol. The solvent of each fraction was evaporated under reduced pressure at 40 °C and monitored using TLC, where a major spot was detected in the 100% methanol fraction. This fraction was purified by elution on sephadex LH-20 column using methanol-water (1:1 v/v) yielding pure white powder compound, Rf value (0.54 in ethyl acetate-methanol-water 100: 16.5: 13.5 v/v/v).

2.4. Animals

Adult male Sprague Dawley rats with (280 ± 30) g were purchased from the animal house of Theodore Bilharz Research Institute (TBRI), Giza, Egypt. The rats were kept in an environmentally controlled room at (20–22) °C, 12 h light/dark cycle and 50%–60% humidity throughout the acclimatization and experimental periods with free access to water and *ad libitum* with rodent food pellet (El-Kahira Company for Oils and Soap, Tanta, Egypt). All experiments conducted followed the international guidelines for animal ethics and were approved by the Institutional Review Board of TBRI.

2.5. Cell culture and treatment

HSC-T6, an immortalized rat hepatic stellate cell line, was a generous gift from Prof. Scott L. Friedman (Division of Liver Diseases, Icahn School of Medicine at Mount Sinai University, New York). Primary isolated hepatocytes were freshly isolated from rats by a two-step portal collagenase perfusion of the liver as previously described [14]. HSCs and hepatocytes were cultured in Dulbecco's Modified Eagle's Medium (DMEM) (Gibco, USA) supplemented with 10% fetal bovine serum (FBS) and 100 U/mL penicillin and 100 µg/mL streptomycin under conditions of 95% air/5% CO_2 at 37 °C. RA was dissolved in a small volume of DMSO (equivalent to <1% of the final volume).

2.5.1. HSCs proliferation/morphology and hepatocyte cytotoxicity assays

Rat HSCs-T6 (5×10^3) were cultured in 96-wells tissue culture plates and treated with various concentrations of RA (0, 25, 50, 100, 200, 400 µg/mL) or vehicle (DMSO, 0.05% final concentration) for 24 and 48 h. The anti-proliferative activity of RA was determined using SRB staining as previously described [15]. Furthermore, HSC morphology was observed under phase-contrast microscope [EVOS® xl core cell culture microscope (Advanced Microscopy Group, USA)].

Cytotoxicity of RA on hepatocytes was determined using MTT assay on freshly rat hepatocytes isolated as described by Mosmann [16], where primary hepatocytes (5×10^3) were cultured in 96-wells tissue culture plates and treated with the same concentrations of RA for 24 h and 48 h.

2.5.2. HSCs activation and apoptosis assays

HSCs activation was assessed via determination of concentrations of TGF-β1 in culture media using the commercial ELISA kits according to the manufacturer's instructions and immunocytostaining of HSCs with α-SMA; moreover, HSCs apoptosis was assessed using caspase-3 immunocytostaining.

Briefly, HSC-T6 cells were seeded on sterile glass slides layered onto the wells of a 6-wells plate and then washed twice with PBS, fixed and stained with α-SMA and caspase-3 respectively according to the manufacturer's instruction.

2.6. Experimental design

Thirty-two rats were randomly divided into four groups (8 rats each): normal control (i); TAA-intoxicated rats injected intraperitoneally (i.p.) with TAA in a dose of 200 mg/kg twice weekly for 12 weeks [17] (ii); TAA-intoxicated rats administered silymarin (iii) or RA (iv) via oral gavage at daily doses of 50 mg/kg [18] and 10 mg/kg [19] respectively for 8 weeks starting from the 5th week of TAA-intoxication where an apparent stage of fibrosis (S2) was recorded, guided by histopathological examination of hepatic tissues. At the end of the experiment, all rats were weighed, killed with an *i.p.w* injection of ketamine (80 mg/kg) and then blood samples were immediately collected where sera were separated for the assessment of liver functions. Livers were dissected and divided into two parts; the first part was fixed in 10% formalin for histopathological and immunohistochemical examinations whereas the second one was washed with 0.9% ice-cold saline and stored at −80 °C until determination of oxidative stress and fibrosis markers.

2.7. Biochemical assays

2.7.1. Liver functions and oxidative stress markers

ALT and AST were determined spectrophotometrically according to Reitman and Frankel [20]. Moreover, the content of reduced glutathione (GSH) and the extent of lipid peroxidation (MDA) were determined in liver homogenates according to the methods described by Ellman [21] and Ohkawa *et al* [22], respectively.

2.7.2. Assessment of fibrosis markers

PDGF-BB, TGF-β1 and TIMP-1 levels were measured in liver tissue homogenates using the commercial ELISA kits. The hepatic content of HP in tissue samples was determined according to Woessner [23]. Briefly, dried liver tissue were hydrolyzed in 6N HCl, and then dissolved in isopropanol and chloramine-T solution followed by reaction with p-dimethylaminobenzaldehyde. The absorbance of the colored product was determined at 540 nm and the amount of HP was expressed as μg/g wet tissue.

2.8. Immunohistopathological assays

2.8.1. Liver histology, inflammation grade and fibrosis stage

Liver specimens embedded in paraffin blocks were sectioned at 4 μm thickness. Slices were then stained with either hematoxylin/eosin (H&E) or Masson's trichrome. The degree septal and portal inflammatory infiltrate were identified according to the criteria set by the Brazilian Society of Pathology and the Brazilian Society of Hepatology (1999) into the following grades: (0) absent or rare portal lymphocytes; (1) discreet increase in the number of portal lymphocytes; (2) moderate increase in the number of portal lymphocytes; (3) marked increase in the number of portal lymphocytes and (4) intense increase in the number of portal lymphocytes.

Moreover, the liver fibrosis area was quantified as described previously [24]. Healthy liver was classified as stage (0): no

fibrosis; stage (1): expansion of fibrosis in portal area localized in perisinusoidal and intralobular fibrosis; stage (2): peripheral fibrosis in portal area, formation of fibrous septum, retention of intralobular architecture; stage (3): fibrous septum accompanied by intralobular structural disorders, no hepatic cirrhosis and stage (4): early hepatic cirrhosis characterized by bridging fibrosis with pseudolobular formation.

2.8.2. Immunohistochemical examinations

Rat liver sections were immunohistochemically examined for IL-6, CD45, α-SMA, caspase-3 and PCNA. Briefly, liver sections were prepared from the paraffin blocks and incubated overnight at 4 °C with anti-rat IL-6, CD45, α-SMA, caspase-3 and PCNA antibodies at the optimal working dilution of 1:100. Slides were sectioned at 4 μm onto positively charged slides (Superfrost plus, Menzel-Glaser, Germany) and the slides were stained on an automated platform (Dako Autostainer Link 48, Denmark). Heat induced antigen retrieval was used for 30 min at 97 °C in the high-PH EnVision™ FLEX Target Retrieval Solution and the primary antibody was used at a dilution of 1:100. The percent of positively stained brown nuclei (PCNA) [25] or brown cytoplasm (IL-6, CD45, α-SMA, and caspase-3) [26] were examined in 10 microscopic fields (at ×400 under Zeiss light microscopy, Jena, Germany).

2.9. Statistical analysis

Data was expressed as mean ± SEM. Statistical analysis was performed either by Student's *t*-test for comparison between two means or by one-way ANOVA test followed by Tukey's as *post hoc* test for multiple comparisons using the GraphPad Prism statistical program (GraphPad Software version 5.03, CA, USA). Differences were considered significant when $P < 0.05$.

3. Results

3.1. Identification of the isolated compound

The isolated compound had UV absorbance at 330 and 294 sh. nm. The ^{1}HNMR and ^{13}CNMR data are shown in Table 1. ^{1}HNMR spectrum of compound RA depicted two doublets at δ 7.42

Table 1
^{1}HNMR and ^{13}CNMR (400 MHz, 100 MHz, DMSO) of compound RA.

| Position	δ_H ppm	δ_C ppm
1	–	127.7
2	7.06 (1H, br.s)	116.7
3	–	143.6
4	–	144.6
5	6.75 (d, 1H, J = 7.8 HZ)	119.8
6	6.98 (1H, dd, J = 7.2, 2.1 Hz)	125.1
7	7.42 (1H, d, J = 16.2 Hz)	148.3
8	6.21 (1H, d, J = 16.2 Hz)	115.9
9	–	165.9
1′	–	127.7
2′	6.69 (br.s, 1H)	119.8
3′	–	145.4
4′	–	145.6
5′	6.61 (1H,d, J = 7.5 Hz)	115.2
6′	6.50 (dd, 1H, J = 7.2, 2.1 Hz)	125.1
7′	2.89 (1H, dd, J = 13.8, 8.8 Hz, 7′a)	36.2
	2.97 (1H, dd, J = 13.8, 8.8, H-7′b)	
8′	4.99 (1H, d, J = 4.8 Hz)	73.3
9′	–	171.0

(J = 16.2 Hz) and 6.21 ppm (J = 16.2 Hz), which on the basis of the observed large proton–proton coupling were assigned to a pair of trans-olefinic protons (H-7 and H-8, respectively). In addition, there were two ABX-spin systems observed in the aromatic region, which were assignable to the three protons of the 3,4-dihydroxyphenyl unit which appeared at δ 6.75 (1H, d, J = 7.8 Hz), 6.98 (1H, dd, J = 7.8, 2.1 Hz) and 7.06 (1H, br.s) assigned to H-5, H-6 and H-2, respectively. Another three protons of the second ABX system appeared at δ 6.50 (1H, d, J = 7.5 Hz), 6.61 (1H, dd, J = 7.2, 2.1 Hz) and 6.69 (1H, br.s), H-6′ refers to δ 6.61, H-5′ refers to δ 6.50 and H-2′ refers to δ 6.69. A doublet in the low field region at δ 4.99 ppm (J = 4.8 Hz) was observed suggesting a proton of a CH group attached to an oxygen-bearing carbon and this was assigned to H-8′. Two doublets, one at δ 2.89 (J = 13.8, 8.8 Hz) and the second at δ 2.98 (J = 13.8, 8.8 Hz) were assigned to the two protons of the 7′-methine group [27].

The ^{13}CNMR spectrum of compound RA showed the characteristic signals of RA especially the presence of two carbonyl carbons, of which one was assigned to a carboxylic acid (δ 171 ppm) and the second of a carboxylic ester (δ 165.9 ppm). The presence of two sets of 3,4-dihydroxyphenyl groups was confirmed by the appearance of 12 aromatic carbons of which four were phenoxy carbons (δ 143.6–145.4 ppm), two olefinic carbons (δ 148.3 and 115.9 ppm), an oxygenated methane carbon at (δ 73.3 ppm) and the other carbon at (δ 36.2 ppm). From the above data, the compound was identified as RA.

3.2. Effect of RA on HSCs proliferation and morphology

RA-treatment mitigated the proliferation of HSC-T6 cells (P < 0.05) in a time and concentration-dependent manner when
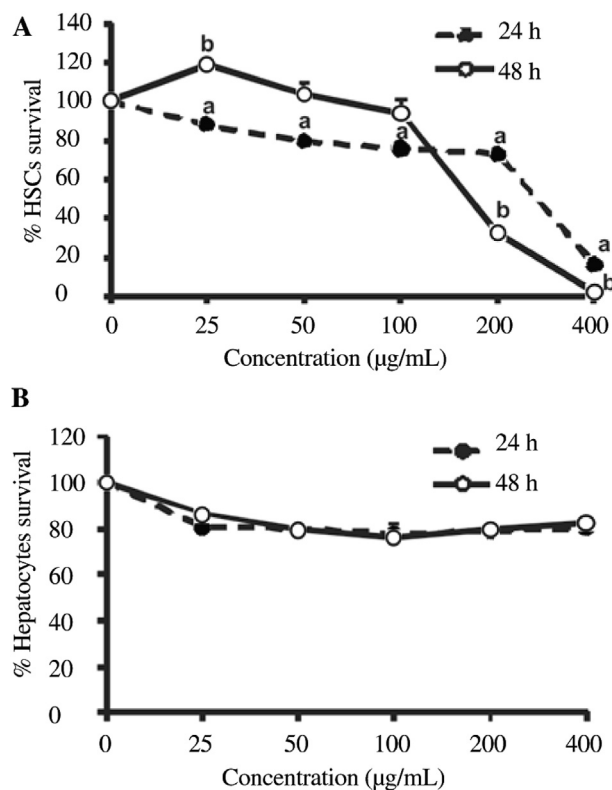
Figure 1. Effect of various concentrations of RA on HSCs proliferation and viability (A) and hepatocytes survival (B).
RA selectively induces HSC cytotoxicity with no signs of toxicity on hepatocytes.

compared to the untreated cells, representing an IC$_{50}$ of 276 µg/mL and 171 µg/mL 24 h and 48 h, respectively (Figure 1A). Adding on, RA showed no impact on hepatocytes (Figure 1B) even after prolonged exposure (up to 48 h) or at higher concentrations (up to 400 µg/mL), indicating that the RA toxicity was specific to HSCs. Accordingly, the concentrations of RA (50, 100, 200 µg/mL) were used in subsequent assays, such concentrations corresponded to approximately $1/4$-, $1/2$-, and 1-fold the IC$_{50}$ after 48 h incubation.

By examining the morphology of HSCs under phase contrast microscope, it was observed that some cells displayed cellular swelling and disintegration while others retained back their quiescent morphological features, which was more pronounced with increased RA concentrations (Figure 2A–D).

3.3. Effect of RA on α-SMA and caspase-3 expression

The exposure of activated HSCs to RA in concentrations of 50, 100 and 200 µg/mL for 48 h resulted in a considerable concentration dependent reduction (P < 0.05) in HSCs activation as advocated by reduction in α-SMA expression by 34.78%, 84.19% and 92.00% respectively in comparison to untreated cells (Figure 2E–H,M). Furthermore, RA resulted in a prominent elevation in caspase-3 expression by 3.5, 7.0 and 7.5 folds when compared to untreated cells denoting an increase in apoptosis (Figure 2I–L,N).

3.4. Effect of RA on TGF-β1 concentrations in culture medium

Treatment of cultured HSCs with RA resulted in a concentration-dependent inhibition (P < 0.05) in TGF-β1 production in culture medium by 7.46% (50 µg/mL), 24.47% (100 µg/mL) and 48.95% (200 µg/mL) when compared to untreated cells (Figure 3) signifying a diminution in HSCs activation.

3.5. Effect of RA on liver function and oxidative stress markers

TAA-intoxication for 12 weeks significantly elevated serum ALT and AST as well as hepatic MDA levels and depleted GSH stores when compared to normal control groups (Table 2). Treatments with either silymarin or RA restored AST and reduced MDA levels (P < 0.05) when compared to TAA-intoxicated groups. In addition, RA restored ALT levels and GSH stores.

3.6. Effect of RA on hepatic fibrosis markers and HP content

Significant increase in hepatic levels of PDGF-BB, TGF-β1, TIMP-1 and HP were observed in TAA-intoxicated rats when compared to normal control rats (Table 2). Hepatic PDGF-BB, TIMP-1 and HP were modulated after silymarin or RA treatments (P < 0.05). Moreover, RA normalized hepatic levels of TGF-β1.

## 3.7. Effect of RA on liver histology

Histological observations of normal liver sections showed preserved architecture with distinct hepatic cells, sinusoidal
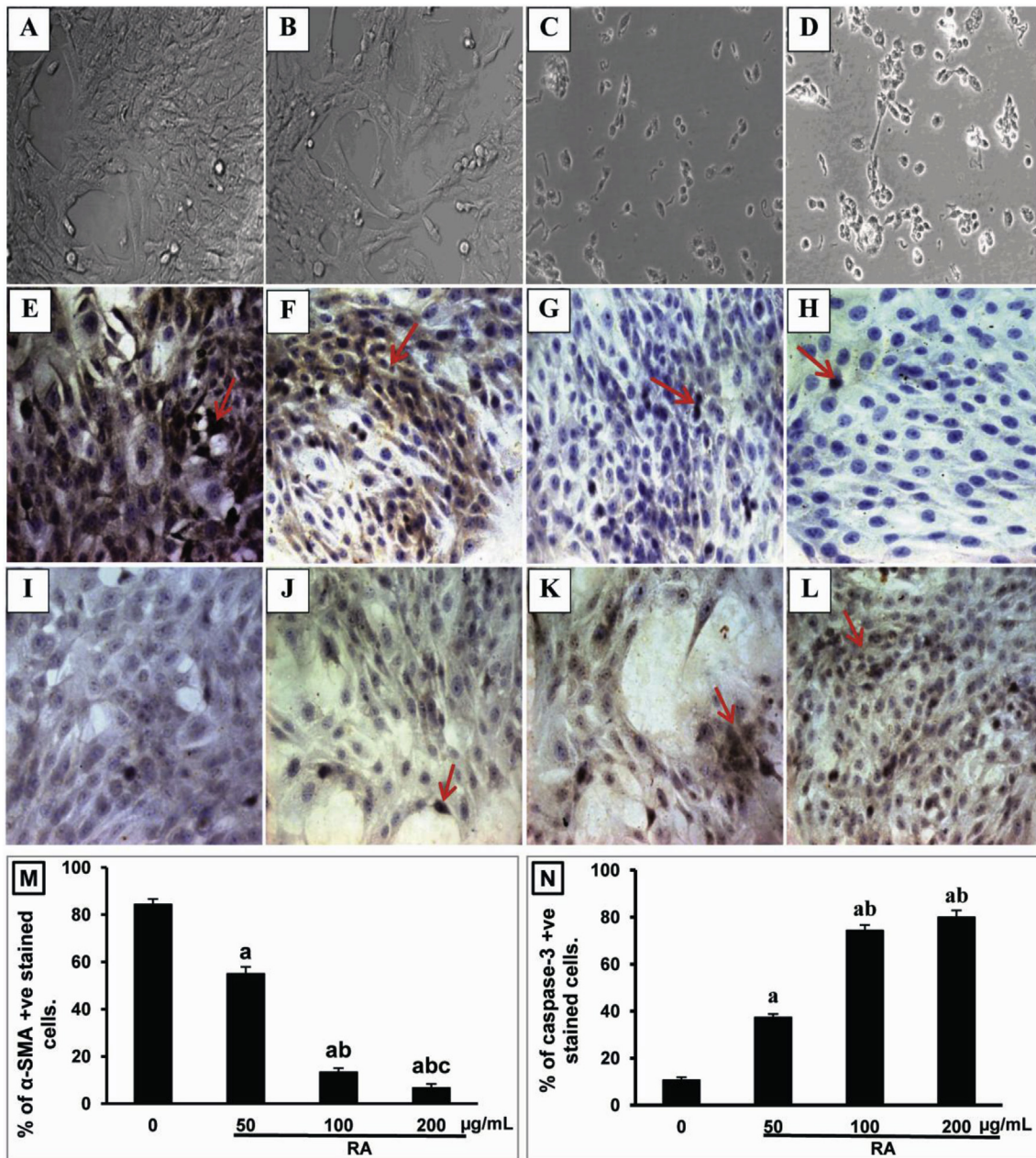
Figure 2. Photomicrographs of cultured untreated HSCs (A, E&I) and those showing their morphological changes, α-SMA and caspase-3 expressions after exposure to RA in a concentration of 50 (B, F&J), 100 (C, G&K) and 200 μg/mL (D, H&L) (corresponding to $^1/_4$, $^1/_2$ and 1 fold of IC50 concentrations) respectively for 48 h (×400).

The expression of α-SMA and caspase-3 were estimated by number of positively stained cells. Data is graphically represented (M&N) as means ± SEM (n = 3). $P < 0.05$ compared with the control group, $P < 0.05$ compared with the corresponding 50 μg/mL concentration, $P < 0.05$ compared with the corresponding 100 μg/mL concentration.
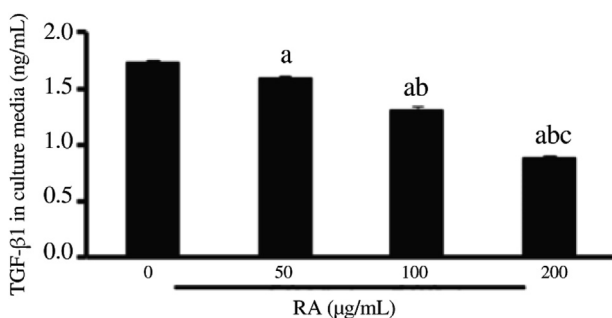
Figure 3. Effect of RA on TGF-β1 production in culture medium.
HSCs were treated with RA (50, 100, 200 μg/mL) for 48 h. All values were represented as means ± SEM (n = 3). [a]$P < 0.05$ compared with the control group; [b]$P < 0.05$ compared with the corresponding 50 μg/mL concentration; [c]$P < 0.05$ compared with the corresponding 100 μg/mL concentration.

spaces and a central vein. The hepatic cells displayed rounded nuclei, uniform cytoplasm with no inflammatory infiltrate (Figure 4A and E). The liver sections of TAA-intoxicated rats revealed disrupted architecture with extensive damage, characterized by sinusoidal dilatation and congestion, centrilobular necrosis (Figure 4B). Marked increase in lymphocyte infiltration was also detected in the portal tract and fibrous septa displaying a lymphocyte infiltration grade of 3.00 ± 0.26 (Figure 4B) associated with the deposition of collagen bundles surrounding the lobules leading to thick fibrotic septa showing a fibrosis score of 3.67 ± 0.21 (Figure 4F).

However, liver recovery was observed in rats administered silymarin as indicated by reduced level of necrosis, mild lymphocyte infiltration with a grade of 0.83 ± 0.17 (Figure 4C)

Table 2

Effect of RA treatment on liver functions, oxidative stress and fibrosis markers in TAA-induced fibrotic rats.

Animal groups	Liver functions		Oxidative stress markers		Fibrosis markers			
	ALT	AST	GSH	MDA	PDGF-BB	TGF-β1	TIMP-1	HP
	(U/L)	(U/L)	(mg/g liver)	(µmol/g liver)	(ng/g liver)	(ng/g liver)	(ng/g liver)	(µg/g liver)
Normal control	55.63 ± 1.96	122.00 ± 5.26	1.50 ± 0.11	18.23 ± 0.89	0.22 ± 0.02	2.98 ± 0.28	1.12 ± 0.04	208.85 ± 10.68
TAA	106.63 ± 3.54^a	162.00 ± 4.83^a	0.48 ± 0.04^a	63.60 ± 2.85^a	0.54 ± 0.03^a	8.37 ± 0.49^a	2.71 ± 0.04^a	826.94 ± 39.35^a
TAA + Silymarin	75.13 ± 4.16^{ab}	136.88 ± 4.71^b	0.96 ± 0.05^{ab}	40.67 ± 4.10^{ab}	0.38 ± 0.01^{ab}	5.25 ± 0.29^{ab}	2.31 ± 0.07^{ab}	434.78 ± 19.27^{ab}
TAA + RA	68.50 ± 4.09^b	133.88 ± 3.26^b	1.38 ± 0.13^{bc}	43.80 ± 2.63^{ab}	0.33 ± 0.02^{ab}	3.32 ± 0.32^{bc}	2.21 ± 0.09^{ab}	439.60 ± 21.77^{ab}

Data are presented as mean ± SEM. ^{a}$P < 0.05$ *vs* normal control group, ^{b}$P < 0.05$ *vs* TAA-intoxicated group, ^{c}$P < 0.05$ *vs* silymarin group. $n = 8$ in groups of liver functions and oxidative stress markers; $n = 6$ in groups of fibrosis markers.
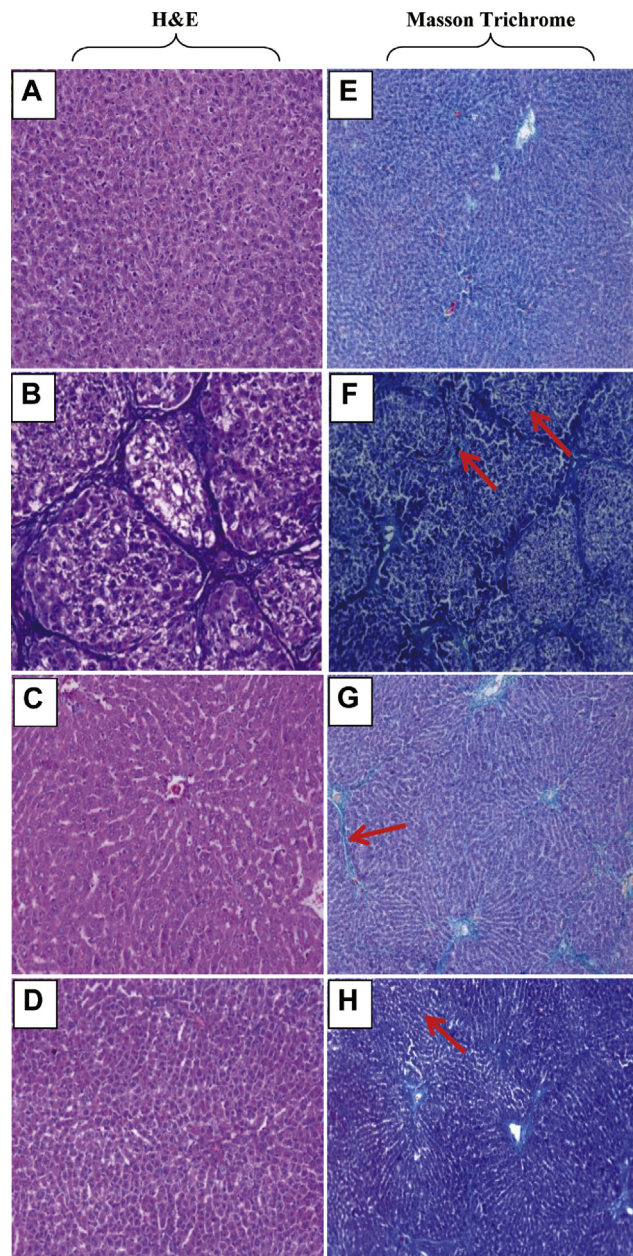
Figure 4. Histopathological examinations.
Hepatic sections stained with H&E (A–D) (×200) and Masson Trichrome (E–H) (×100) of normal (A&E), TAA (B&F), silymarin (C&G) and RA-treated rats (D&H). $n = 6$ in each group. The fibrosis in the liver sections is shown as red arrows.

and only few thin short bundles of collagen showing a fibrosis score of 1.83 ± 0.31 (Figure 4G). Better liver recovery was observed in rats administered RA where the hepatic architecture appeared intact, exhibiting barely few lymphocyte infiltration (grade of 0.50 ± 0.22) with almost normal hepatocytes (Figure 4D) showing a fibrosis score of 1.17 ± 0.41 (Figure 4H).
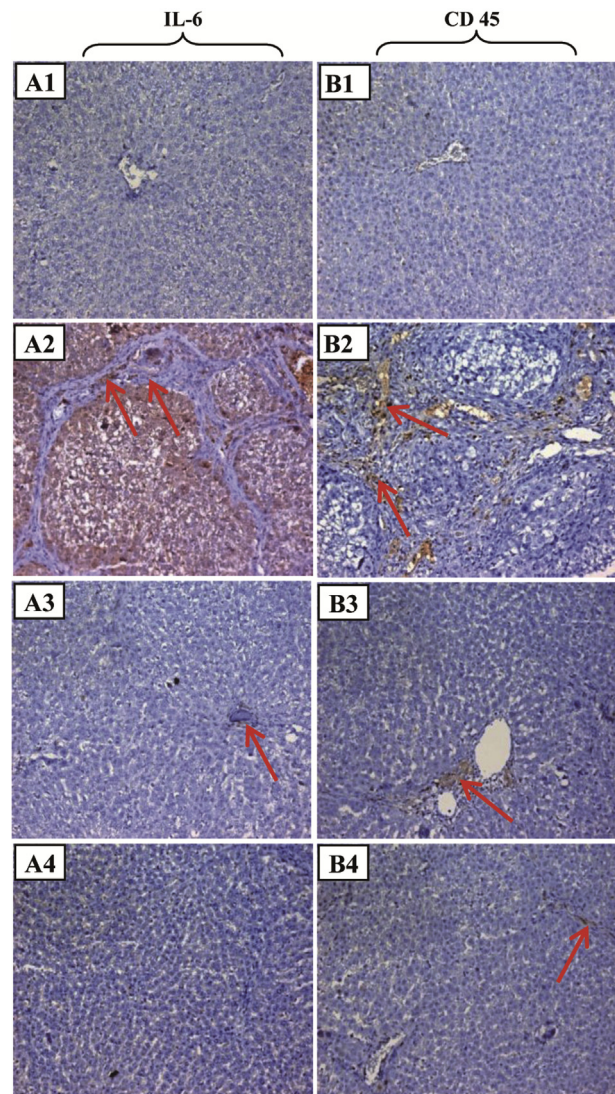
Figure 5. Immunohistochemical examinations of IL-6 and CD45 expressions in rat liver sections of normal, TAA, silymarin and RA-treated rats. A1–A4: ×200; B1–B4: ×200; $n = 6$ in each group.

### 3.8. Effect of RA on IL-6, CD45, PCNA, α-SMA and caspase-3 by IHC

The anti-inflammatory effect of RA was evaluated via IHC expression of IL-6 in hepatic tissues (Figure 5A1–A4). TAA-intoxication for 12 weeks resulted in a substantial elevation in IL-6 expression that was located mostly in cytoplasm of hepatocytes in portal tract and fibrous septa (Figure 5A2) when compared to normal control group (Figure 5A1). IL-6 expression was explicitly suppressed by RA treatment (Figure 5A4), which as well revealed an upper hand in the suppression of elevated IL-6 over silymarin (Figure 5A3). Such finding suggested that RA inhibited the inflammatory response induced by TAA-intoxication.

To assess the infiltration of lymphocytes, lymphocytes were stained for the CD45 antigen (Figure 5B1–B4), where TAA-intoxicated livers were infiltrated by lymphocytes in the portal tract and fibrous septa (Figure 5B2). This inflammatory response was significantly affected by RA administration as exemplified by milder lymphocyte infiltration (Figure 5B4) when compared to silymarin (Figure 5B3).

The degree of hepatocytes proliferation was analyzed using IHC staining for PCNA (Figure 6A), which was expressed at a low basal level in hepatocytes of untreated control (Figure 6A1). Conversely, its expression was up-regulated in hepatocytes of TAA-intoxicated rats, which indicated a pronounced proliferation to repair the damaged liver tissues (Figure 6A2). Silymarin distinctly ($P < 0.05$) diminished the proliferation of damaged hepatocytes (Figure 6A3), while RA administration efficiently halted the proliferation of impaired hepatocytes (Figure 6A4).

Figure 6B2 illustrated the marked elevation of α-SMA protein expression in liver tissues of TAA-intoxicated rats when compared to control rats (Figure 6B1), this was distinguished in areas of centrilobular and periportal fibrotic bands. Treatment
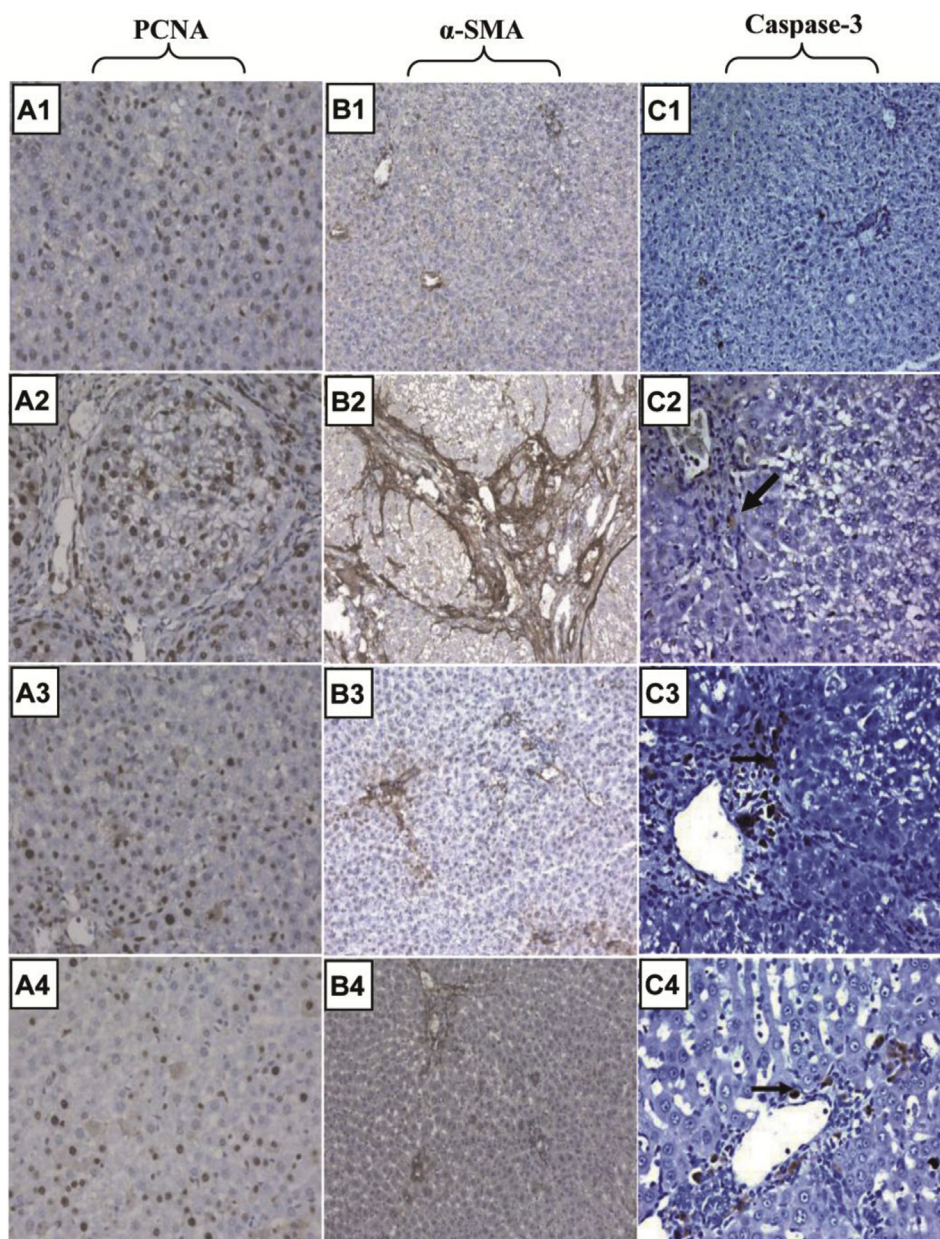
Figure 6. Immunohistochemical examinations of PCNA, α-SMA and caspase-3 expressions in rat liver sections of normal, TAA, silymarin and RA-treated rats.
A1–A4: ×400; B1–B4: ×200; C1: ×200; C2–C4: ×400. *n* = 6 in each group.

with either silymarin (Figure 6B3) or RA (Figure 6B4) notably modulated α-SMA protein expression when compared to TAA-intoxicated group.

Examination of caspase-3 immunostained liver sections of normal (Figure 6C1) and those intoxicated with TAA (Figure 6C2) showed negatively and few caspase-3 positive cells respectively. However, liver sections treated with either silymarin (Figure 6C3) or RA (Figure 6C4) revealed increased expression ($P < 0.05$) in caspase-3 positive cells in portal and periportal areas where collagen deposition was observed.

4. Discussion

Despite the progress in modern medicine, up till now, there is no successful therapeutic approach regarding the treatment of liver fibrosis [28]. Silymarin, positive control used in this research, has been widely used as a hepatoprotective in treatment of patients with liver diseases [29] besides, its anti-fibrotic effects were recorded in experimental animals [30,31]. However, it has shown some limitations regarding the treatment of chronic liver impairment such as cirrhosis; also, gastroenteritis was recorded in some patients [32]. Accordingly, it is essential to find effective pharmaceuticals for the treatment of hepatic fibrosis with high safety margin. The use of natural products in the treatment of hepatic diseases was traced over decades due to their abundance, low cost and few adverse effects [28]. The present study was conducted to investigate the potential antifibrotic effects of RA on HSCs *in vitro* and in TAA-induced liver fibrosis animal model.

The *in vitro* results revealed that RA significantly inhibited the proliferation of HSC-T6 cells in a time- and concentration-dependent manner without impairing the parenchymal cell viability, which is in agreement with Zhang *et al* [33]. Such recorded anti-proliferative effects could probably be attributed to the correlation between the pro-oxidant and cytotoxic activities of RA; a dietary polyphenolic compound, leading to the acceleration of lipid peroxidation and/or induction of DNA damage [34], suggesting that RA could partly halt hepatic fibrosis progression. It has also been documented that polyphenols selectively induce oxidative damage and cytotoxic effects on HSCs without any recorded hepatocytes cytotoxicity due to the increased expression of the antioxidant enzyme catalase in primary rat hepatocytes than activated HSCs [35,36].

In the present study, chronic TAA-intoxication for 12 weeks caused micro and macronodular hepatic fibrosis as histopathologically portrayed. Liver injury was also verified by extensive increase in serum ALT and AST levels that resulted from their leakage from damaged TAA-intoxicated tissues [37]. RA treatment lowered both ALT and AST levels, thus maintaining liver cell membrane integrity.

Free radicals are believed to play a major role in the development of TAA-induced liver fibrosis [38], which is mediated through lipid peroxidation and depletion of antioxidants [39]. Likewise, TAA-intoxication caused a prominent elevation in the hepatic expression of IL-6, one of the most pivotal pro-inflammatory cytokines [40], thus indicating a pronounced inflammatory state, which is in coherence with previous studies [41,42]. In support of our results, previous studies reported that upon chronic injury the fibrotic process is associated with tissue inflammation and oxidative stress [43]. Herein, results demonstrated the protective effects of RA treatment against hepatic inflammation as elucidated by

efficient reduction in the expression of IL-6. This was further confirmed by the prominent reduction in the hepatic inflammatory score and lymphocyte count. RA as well counteracted TAA-induced oxidative stress through down-regulation of reactive oxygen species (ROS). This is indicated by reduced level of MDA and replenishment of GSH stores, thereby protecting hepatocytes against ROS.

Furthermore, the free radicals resulting from TAA metabolism precedes the activation of HSCs, which in turn secrete fibrinogen and growth factors leading to the progression of acute liver injury towards liver fibrosis [44]. Among the growth factors, TGF-β1 and PDGF-BB are considered to be the most potent profibrogenic cytokines in liver fibrogenesis [45,46]. They are both generated from damaged hepatocytes, activated Kupffer cells and platelets, hence inducing HSCs activation and proliferation [47] as well as amplifying α-SMA expression [48]. Similarly, the recorded *in vitro* results revealed that RA treatment reduced TGF-β1 production in culture media in a concentration-dependent manner, the number of activated HSCs as well as the expression of α-SMA. Such results were in accordance with the *in vivo* findings where RA treatment alleviated the upregulated hepatic TGF-β1 and PDGF-BB levels as well as α-SMA expression that resulted from long-term administration of TAA, elucidating an improvement in the pathological damage induced by oxidative stress.

Additionally, HSCs activation act as the main source of excessive ECM production and deposition where activated HSCs synthesize TIMPs thus causing further increase in collagen deposition mainly collagen type I [49,50]. The authors also added that TAA-intoxication caused a dramatic increase in hepatic levels of TIMP-1 and HP content reflecting an increase in the amount of collagen deposited. These results were supported by the presence of fibrosis (S4) and numerous collagen strands. RA treatment reduced TIMP-1 and HP levels, consequently diminishing collagen deposition in the liver of fibrotic rats (S1), which might help in regression of liver fibrosis.

The current study indicated that RA did not only inhibit the activation or proliferation of HSCs, but also triggered the apoptosis of these cells in animals' hepatic tissues as signified by increased caspase-3 expression; since induction of HSCs apoptosis has become potentially important in prevention or treatment of hepatic fibrosis [51]. These results were extra confirmed and extended through the *in vitro* observations. Additionally, the increase in apoptosis might be related to the downregulation of TIMP-1 levels as reported herein since it was observed that overexpression of TIMP-1 was correlated with failure of activated HSCs to undergo apoptosis resulting in downregulation of caspases [52,53].

Moreover, the proliferative activity of hepatocytes was investigated via PCNA staining, which reflects the activity of chronic liver disease [54]. Herein, RA inhibited the proliferation of damaged hepatocytes as verified by the alleviation of PCNA staining when compared to the higher damage and PCNA upregulation in the fibrotic animals.

In conclusion, the *in vitro* results revealed that RA suppressed the proliferation and activation of cultured HSCs accompanied with triggering of their apoptosis. Interestingly, RA reversed the activated HSCs morphology back to their quiescent form. Such results were further enforced by the *in vivo* findings where the administration of RA to chronically TAA-intoxicated rats led to the reduction of HSCs proliferation, activation, collagen deposition and fibrosis score (S1 *vs* S4). RA

treatment as well induced the apoptosis of HSCs and inhibited the proliferation of damaged hepatocytes. Additionally, RA exerted advantageous benefits over silymarin in terms of improvement of hepatic GSH stores, reduction in serum ALT, hepatic TGF-β1 levels, expressions of inflammatory markers (IL-6 and CD45) and PCNA reflecting hepatocyte regeneration and progression towards fibrosis reversal. These findings revealed the therapeutic potential of RA against hepatic fibrosis, although more clinical studies are demanded to verify its therapeutic efficacy in humans.

Conflict of interest statement

The authors declare that they have no conflict of interest.

Acknowledgements

References

[1] Ramachandran P, Iredale JP. Liver fibrosis: a bidirectional model of fibrogenesis and resolution. *QJM* 2012; **105**(9): 813-817.

[2] Bohanon FJ, Wang X, Ding C, Ding Y, Radhakrishnan GL, Rastellini C, et al. Oridonin inhibits hepatic stellate cell proliferation and fibrogenesis. *J Surg Res* 2014; **190**(1): 55-63.

[3] Friedman SL. Mechanisms of hepatic fibrogenesis. *Gastroenterology* 2008; **134**(6): 1655-1669.

[4] Brenner DA. Molecular pathogenesis of liver fibrosis. *Trans Am Clin Climatol Assoc* 2009; **120**: 361-368.

[5] Atzori L, Poli G, Perra A. Hepatic stellate cell: a star cell in the liver. *Int J Biochem Cell Biol* 2009; **41**(8–9): 1639-1642.

[6] Hauff P, Gottwald U, Ocker M. Early to phase Ⅱ drugs currently under investigation for the treatment of liver fibrosis. *Expert Opin Investig Drugs* 2015; **24**(3): 309-327.

[7] Frenzel C, Teschke R. Herbal hepatotoxicity: clinical characteristics and listing compilation. *Int J Mol Sci* 2016; **17**(5): 588.

[8] Soares HD. The use of mechanistic biomarkers for evaluating investigational CNS compounds in early drug development. *Curr Opin Investig Drugs* 2010; **11**(7): 795-801.

[9] Petersen M, Simmonds MS. Rosmarinic acid. *Phytochemistry* 2003; **62**(2): 121-125.

[10] Chu X, Ci X, He J, Jiang L, Wei M, Cao Q, et al. Effects of a natural prolyl oligopeptidase inhibitor, rosmarinic acid, on lipopolysaccharide-induced acute lung injury in mice. *Molecules* 2012; **17**(3): 3586-3598.

[11] Gao LP, Wei HL, Zhao HS, Xiao SY, Zheng RL. Antiapoptotic and antioxidant effects of rosmarinic acid in astrocytes. *Pharmazie* 2005; **60**(1): 62-65.

[12] Huang SS, Zheng RL. Rosmarinic acid inhibits angiogenesis and its mechanism of action *in vitro*. *Cancer Lett* 2006; **239**(2): 271-280.

[13] Moon DO, Kim MO, Lee JD, Choi YH, Kim GY. Rosmarinic acid sensitizes cell death through suppression of TNF-alpha-induced NF-kappaB activation and ROS generation in human leukemia U937 cells. *Cancer Lett* 2010; **288**(2): 183-191.

[14] Seglen PO. Preparation of isolated rat liver cells. *Methods Cell Biol* 1976; **13**: 29-83.

[15] Skehan P, Storeng R, Scudiero D, Monks A, McMahon J, Vistica D, et al. New colorimetric cytotoxicity assay for anticancer-drug screening. *J Natl Cancer Inst* 1990; **82**(13): 1107-1112.

[16] Mosmann T. Rapid colorimetric assay for cellular growth and survival: application to proliferation and cytotoxicity assays. *J Immunol Methods* 1983; **65**(1–2): 55-63.

[17] Aydin AF, Küskü-Kiraz Z, Doğru-Abbasoğlu S, Güllüoğlu M, Uysal M, Koçak-Toker N. Effect of carnosine against thioacetamide-induced liver cirrhosis in rat. *Peptides* 2010; **31**(1): 67-71.

[18] Kadir FA, Kassim NM, Abdulla MA, Yehye WA. Hepatoprotective role of ethanolic extract of *Vitex negundo* in thioacetamide-induced liver fibrosis in male rats. *Evid Based Complement Altern Med* 2013; **2013**: 739850.

[19] Gamaro GD, Suyenaga E, Borsoi M, Lermen J, Pereira P, Ardenghi P. Effect of rosmarinic and caffeic acids on inflammatory and nociception process in rats. *ISRN Pharmacol* 2011; **2011**: 451682.

[20] Reitman S, Frankel S. A colorimetric method for the determination of serum glutamic oxaloacetic and glutamic pyruvic transaminases. *Am J Clin Pathol* 1957; **28**: 56-63.

[21] Ellman GL. Tissue sulfhydryl groups. *Arch Biochem Biophys* 1959; **82**(1): 70-77.

[22] Ohkawa H, Ohishi N, Yagi K. Assay for lipid peroxides in animal tissues by thiobarbituric acid reaction. *Anal Biochem* 1979; **95**(2): 351-358.

[23] Woessner JF Jr. The determination of hydroxyproline in tissue and protein samples containing small proportions of this imino acid. *Arch Biochem Biophys* 1961; **93**: 440-447.

[24] Li L, Hu Z, Li W, Hu M, Ran J, Chen P, et al. Establishment of a standardized liver fibrosis model with different pathological stages in rats. *Gastroenterol Res Pract* 2012; **2012**: 560345.

[25] Shen HW, Yi L, Wang XM, Yao MJ, Deng JW, Fang JZ, et al. Expression of Caspase-3 and Bcl-2 in bladder transitional carcinoma and their significance. *Ai Zheng* 2004; **23**(2): 181-184.

[26] Atta HM, Al-Hendy A, Salama SA, Shaker OG, Hammam OA. Low dose simultaneous delivery of adenovirus encoding hepatocyte growth factor and vascular endothelial growth factor in dogs enhances liver proliferation without systemic growth factor elevation. *Liver Int* 2009; **29**(7): 1022-1030.

[27] Lu Y, Foo LY. Rosmarinic acid derivatives from *Salvia officinalis*. *Phytochemistry* 1999; **51**: 91-94.

[28] Madrigal-Santillan E, Madrigal-Bujaidar E, Alvarez-Gonzalez I, Sumaya-Martínez MT, Gutiérrez-Salinas J, Bautista M, et al. Review of natural products with hepatoprotective effects. *World J Gastroenterol* 2014; **20**(40): 14787-14804.

[29] Dryden GW, Song M, McClain C. Polyphenols and gastrointestinal diseases. *Curr Opin Gastroenterol* 2006; **22**(2): 165-170.

[30] Chong LW, Hsu YC, Chiu YT, Yang KC, Huang YT. Antifibrotic effects of thalidomide on hepatic stellate cells and dimethylnitrosamine-intoxicated rats. *J Biomed Sci* 2006; **13**(3): 403-418.

[31] Hsu YC, Chiu YT, Lee CY, Wu CF, Huang YT. Anti-fibrotic effects of tetrandrine on bile-duct ligated rats. *Can J Physiol Pharmacol* 2006; **84**(10): 967-976.

[32] Muriel P, Rivera-Espinoza Y. Beneficial drugs for liver diseases. *J Appl Toxicol* 2008; **28**(2): 93-103.

[33] Zhang JJ, Wang YL, Feng XB, Song XD, Liu WB. Rosmarinic acid inhibits proliferation and induces apoptosis of hepatic stellate cells. *Biol Pharm Bull* 2011; **34**(3): 343-348.

[34] de la Lastra CA, Villegas I. Resveratrol as an antioxidant and pro-oxidant agent: mechanisms and clinical implications. *Biochem Soc Trans* 2007; **35**(Pt 5): 1156-1160.

[35] Hsieh SC, Wu CH, Wu CC, Yen JH, Liu MC, Hsueh CM, et al. Gallic acid selectively induces the necrosis of activated hepatic stellate cells via a calcium-dependent calpain I activation pathway. *Life Sci* 2014; **102**(1): 55-64.

[36] Chang YJ, Hsu SL, Liu YT, Lin YH, Lin MH, Huang SJ, et al. Gallic acid induces necroptosis via TNF-α signaling pathway in activated hepatic stellate cells. *PLoS One* 2015; **10**(3): e0120713.

[37] Ajith TA, Hema U, Aswathy MS. *Zingiber officinale* Roscoe prevents acetaminophen-induced acute hepatotoxicity by enhancing hepatic antioxidant status. *Food Chem Toxicol* 2007; **45**(11): 2267-2272.

[38] Lukivskaya O, Patsenker E, Lis R, Buko VU. Inhibition of inducible nitric oxide synthase activity prevents liver recovery in rat thioacetamide-induced fibrosis reversal. *Eur J Clin Investig* 2008; **38**(5): 317-325.

[39] Sugino H, Kumagai N, Watanabe S, Toda K, Takeuchi O, Tsunematsu S, et al. Polaprezinc attenuates liver fibrosis in a mouse model of non-alcoholic steatohepatitis. *J Gastroenterol Hepatol* 2008; **23**(12): 1909-1916.

[40] Wen Y, Feng D, Wu H, Liu W, Li H, Wang F, et al. Defective Initiation of liver regeneration in osteopontin-deficient mice after partial hepatectomy due to insufficient activation of IL-6/stat3 pathway. *Int J Biol Sci* 2015; **11**(10): 1236-1247.

[41] Tsai MK, Lin YL, Huang YT. Effects of salvianolic acids on oxidative stress and hepatic fibrosis in rats. *Toxicol Appl Pharmacol* 2010; **242**(2): 155-164.

[42] Weng TC, Shen CC, Chiu YT, Lin YL, Huang YT. Effects of armepavine against hepatic fibrosis induced by thioacetamide in rats. *Phytother Res* 2012; **26**(3): 344-353.

[43] Kisseleva T, Brenner DA. Mechanisms of fibrogenesis. *Exp Biol Med* 2008; **233**(2): 109-122.

[44] Bassiouny AR, Zaky AZ, Abdulmalek SA, Kandeel KM, Ismail A, Moftah M. Modulation of AP-endonuclease1 levels associated with hepatic cirrhosis in rat model treated with human umbilical cord blood mononuclear stem cells. *Int J Clin Exp Pathol* 2011; **4**(7): 692-707.

[45] Borkham-Kamphorst E, van Roeyen CR, Ostendorf T, Floege J, Gressner AM, Weiskirchen R. Pro-fibrogenic potential of PDGF-D in liver fibrosis. *J Hepatol* 2007; **46**(6): 1064-1074.

[46] Zhou J, Zhong DW, Wang QW, Miao XY, Xu XD. Paclitaxel ameliorates fibrosis in hepatic stellate cells via inhibition of TGF-beta/Smad activity. *World J Gastroenterol* 2010; **16**(26): 3330-3334.

[47] Tacke F, Weiskirchen R. Update on hepatic stellate cells: pathogenic role in liver fibrosis and novel isolation techniques. *Expert Rev Gastroenterol Hepatol* 2012; **6**(1): 67-80.

[48] Gressner AM, Weiskirchen R. Modern pathogenetic concepts of liver fibrosis suggest stellate cells and TGF-b as major players and therapeutic targets. *J Cell Mol Med* 2006; **10**(1): 76-99.

[49] Gabele E, Brenner DA, Rippe RA. Liver fibrosis: signals leading to the amplification of the fibrogenic hepatic stellate cell. *Front Biosci* 2003; **8**: d69-77.

[50] Tsukada S, Parsons CJ, Rippe RA. Mechanisms of liver fibrosis. *Clin Chim Acta* 2006; **364**(1–2): 33-60.

[51] Guicciardi ME, Gores GJ. Apoptosis as a mechanism for liver disease progression. *Semin Liver Dis* 2010; **30**(4): 402-410.

[52] Preaux AM, D'Ortho MP, Bralet MP, Laperche Y, Mavier P. Apoptosis of human hepatic myofibroblasts promotes activation of matrix metalloproteinase-2. *Hepatology* 2002; **36**(3): 615-622.

[53] Liu XW, Bernardo MM, Fridman R, Kim HR. Tissue inhibitor of metalloproteinase-1 protects human breast epithelial cells against intrinsic apoptotic cell death via the focal adhesion kinase/phosphatidylinositol 3-kinase and MAPK signaling pathway. *J Biol Chem* 2003; **278**(41): 40364-40372.

[54] Nakajima T, Kagawa K, Ueda K, Ohkawara T, Kimura H, Kakusui M, et al. Evaluation of hepatic proliferative activity in chronic liver diseases and hepatocellular carcinomas by proliferating cell nuclear antigen (PCNA) immunohistochemical staining of methanol-fixed tissues. *J Gastroenterol* 1994; **29**(4): 450-454.